

HIGH TEMPERATURE (600°C - 800°C)  
THERMALLY ACTIVATED DEFORMATION BEHAVIOUR  
OF  $\alpha$ -ZIRCALOY-4-OXYGEN ALLOYS

by

BHOLA N. MEHROTRA

A THESIS SUBMITTED TO THE FACULTY OF GRADUATE STUDIES  
IN PARTIAL FULFILLMENT OF THE REQUIREMENTS FOR THE DEGREE  
OF MASTER OF SCIENCE IN MECHANICAL ENGINEERING

DEPARTMENT OF MECHANICAL ENGINEERING  
UNIVERSITY OF MANITOBA  
WINNIPEG, MANITOBA

FEBRUARY, 1979



HIGH TEMPERATURE (600°C - 800°C)  
THERMALLY ACTIVATED DEFORMATION BEHAVIOUR  
OF  $\alpha$ -ZIRCALOY-4-OXYGEN ALLOYS

BY

BHOLA N. MEHROTRA

A dissertation submitted to the Faculty of Graduate Studies of  
the University of Manitoba in partial fulfillment of the requirements  
of the degree of

MASTER OF ENGINEERING

©1979

Permission has been granted to the LIBRARY OF THE UNIVERSITY OF MANITOBA to lend or sell copies of this dissertation, to the NATIONAL LIBRARY OF CANADA to microfilm this dissertation and to lend or sell copies of the film, and UNIVERSITY MICROFILMS to publish an abstract of this dissertation.

The author reserves other publication rights, and neither the dissertation nor extensive extracts from it may be printed or otherwise reproduced without the author's written permission.

## TABLE OF CONTENTS

	<u>Page</u>
ABSTRACT . . . . .	i
ACKNOWLEDGEMENTS . . . . .	ii
LIST OF FIGURES . . . . .	iii
LIST OF TABLES . . . . .	vi
1. INTRODUCTION & OBJECTIVES . . . . .	1
2. LITERATURE SURVEY . . . . .	7
2.1 Plastic Flow of Metals . . . . .	7
2.1.1 Thermal and athermal obstacles . . . . .	7
2.1.2 Thermodynamics of dislocation glide . . . . .	12
2.1.3 Experimental determination of activation parameters . . . . .	17
2.2 Solid Solution Hardening . . . . .	28
2.2.1 Introduction . . . . .	28
2.2.2 Effect of temperature, solute concentration and solute characteristics . . . . .	30
2.2.3 The analysis of solid solution hardening . . . . .	31
2.3 Literature on Zirconium and its Oxygen Alloys . . . . .	31
2.3.1 Deformation behaviour . . . . .	32
2.3.2 Solid solution hardening of Zr-0 alloys . . . . .	38
2.3.3 Deformation Behaviour of Zircaloy-2 and Zircaloy-4 . . . . .	39

	<u>Page</u>
3. EXPERIMENTAL METHODS . . . . .	41
3.1 Material . . . . .	41
3.2 Tensile Samples Preparation . . . . .	41
3.3 Tensile Testing . . . . .	46
4. RESULTS . . . . .	49
4.1 Effect of Oxygen Content on Y.S. (0.2%), m, $\tau^*$ , $\tau_\mu$ , $V^*$ and $\Delta G_O^\mu$ . . . . .	50
4.2 Effect of Temperature on $\tau_{0.2\%}$ , m, $\tau^*$ , $\tau_\mu$ , $V^*$ and $\Delta G^\mu$ . . . . .	63
5. DISCUSSION . . . . .	77
5.1 Identification of Rate Controlling Mechanism . . . . .	77
5.2 Role of Oxygen . . . . .	86
5.3 Atypical Temperature Dependence of $\tau_\mu/\mu$ and $\Delta G^\mu$ . . . . .	89
6. SUMMARY AND CONCLUSIONS . . . . .	93
SUGGESTIONS FOR FUTURE WORK . . . . .	95
REFERENCES . . . . .	96

ABSTRACT

The high temperature thermally activated deformation behaviour of Zircaloy-4-Oxygen alloys containing oxygen up to 1 wt % has been investigated. A decremental unloading technique (Dip technique) was employed to determine the internal stress ( $\tau_{\mu}$ ) and thus the effective stress ( $\tau^*$ ). Strain rate change tests were done to determine strain rate sensitivity ( $m$ ) and activation volume ( $V^*$ ). The activation energy ( $\Delta G^{\mu}$ ) was calculated from the above data. Oxygen was found to produce an increase in Y.S. (0.2%),  $\tau^*$  and  $\Delta G_0^{\mu}$  and a decrease in  $m$  and  $V^*$  while  $\tau_{\mu}$  was not affected significantly.

These experimental results support the view that the predominant rate controlling mechanism for deformation in this temperature regime is the thermally activated breaking of attractive junctions for these alloys. Oxygen atoms, pairs or clusters of oxygen atoms, are ruled out as barriers, instead the strengthening is attributed to an increase in the core width of the dislocations due to the presence of oxygen. This in turn results in a more stable attractive junction, which is reflected in the increasing values of  $\Delta G_0^{\mu}$  with increase in oxygen. Finally it is suggested that the atypical temperature dependence of  $\tau_{\mu}/\mu$  and  $\Delta G^{\mu}$  is a direct consequence of dynamic recovery.

ACKNOWLEDGEMENT

The author wishes to express his deep gratitude to Professor K. Tangri for his continued help and advice which was sought throughout this work. Many thanks are also extended to Drs. H.E. Rosinger (AECL, Pinawa), O.T. Woo (AECL, Chalk River) and D. Tseng for their helpful comments. The acknowledgements are also due to Mr. John VanDorp for constructing the tensile jig. My deepest appreciation is due to dear friends, especially to Arvind and Maninder for their suggestions and encouragement.

This work was financially supported by the Atomic Energy of Canada Research Company, Pinawa, Canada. The author also appreciates the financial support provided by The University of Manitoba. Thanks are again due to Dr. Rosinger for the supply of Zircaloy-4 alloys and also for the oxygen analysis.

I am grateful to my family members, whose inspiration and well wishes were always needed for the completion of the project. Lastly, but not least, the acknowledgements are due to Mrs. P. Giardino for her quick and careful typing, which expedited the submission of this thesis.

LIST OF FIGURES

<u>FIGURE</u>		<u>Page</u>
1	Pseudobinary Zr-4-0 Phase Diagram . . . . .	4
2	Schematic Diagram Showing the Variation of the Stress with Temperature and Strain Rate and also the Partition of Thermal and Athermal Stress . . . . .	8
3a	Stress-Distance Curves for Typical Long and Short Range Interactions . . . . .	11
3b	Schematic Diagram Illustrating Long and Short Range Stress Fields Encountered by a Moving Dislocation . . . . .	11
4a	Schematic Diagram of a Dislocation Held up at a Short Range Barrier and Acted by an Effective Stress . . . . .	14
4b	Square-topped Approximation to the Force-Distance Curve . . . . .	14
5	Schematic Diagram of the Temperature Dependence of Flow Stress in Metals . . . . .	18
6a	Schematic Illustration of the Stress-Relaxation Test . . . . .	21
6b	Decremental Unloading Version of the Stress-Relaxation Test . . . . .	21
7	Change of Strain Rate in a Tensile Test . . . . .	26
8a	Determination of Total Activation Energy by Extrapolation of $\Delta G$ vs $\tau^*$ Curve to $\tau^* = 0$ . . . . .	27
8b	Determination of Total Activation Energy by Extrapolation of $\Delta G$ vs $T$ Curve to $T = T_0$ . . . . .	27
9	Microstructure of Zr-4-0.75 Wt%O Alloy . . . . .	45
10	The Loading Fixture . . . . .	47

<u>FIGURE</u>	<u>Page</u>
11 Schematic of Testing Procedure . . . . .	48
12 A Typical Set of Engg. Stress ( $\sigma$ ) - Engg. Strain ( $\epsilon$ ) Curves for Zircaloy-4 (0.60 Wt%O) Specimens Deformed Between 600°C and 800°C . . . . .	51
13 Effect of Oxygen Concentration on 0.2% Yield Stress ( $\sigma$ ) of Zircaloy-4 at Temperatures Ranging from 600°C - 800°C . . . . .	54
14 The Strain Rate Sensitivity ( $m$ ) as a Function of Oxygen Concentration for Zr-4 at Temperatures 600°C - 800°C . . . . .	56
15 Effect of Oxygen Concentration on the Thermal Component ( $\tau^*$ ) of Flow Stress for Zr-4 at all Temperatures . . . . .	57
16 The Modulus Corrected Internal Stress ( $\tau_{\mu}/\mu$ ) Plotted as a Function of Oxygen Content for all Temperatures . . . . .	58
17 The Activation Volume ( $V^*$ ) as a Function of Oxygen Content in the Temperature Range of 600°C - 800°C . . . . .	62
18 The Plot of the Activation Energy ( $\Delta G_0^{\mu}$ ) as a Function of Oxygen Content . . . . .	67
19 The Temperature Dependence of Modulus Corrected Flow Stress (0.2%) for all Zr-4-Oxygen Alloys (0.12 - 1.00 Wt%O). . . . .	68
20 The Temperature Dependence of Strain Rate Sensitivity for all Alloys . . . . .	69
21 The Variation in the Effective Stress ( $\tau^*$ ) as a Function of Temperature Over the Range 600°C to 800°C for all Alloys . . . . .	70
22 The Temperature Dependence of $\tau_{\mu}/\mu$ for all Alloys Over the Temperature Range 600°C to 800°C . . . . .	71
23 The Effect of Temperature on the Activation Volume ( $V^*$ ) of Zircaloy-4- Oxygen Alloys . . . . .	73



<u>FIGURE</u>		<u>Page</u>
24	The Effect of Temperature on the Activation Energy ( $\Delta G^H$ ) of Zircaloy-4 and its Oxygen Alloys . . . . .	74
25	Schematic Diagram of (a) Climb of Edge Dislocation (b) Non-Conservative Motion of Jogged Screw Dislocation (c) Cross-Slipping . . . . .	79
26	Effect of Temperature on the Effective Stress ( $\tau^*$ ) of Zircaloy-4-Oxygen Alloys to Examine the Mechanism of Cross-Slip . . . . .	83
27	(a) Formation of an Attractive Junction xy (b) Schematic Representation of the Attractive Junction for the Case of Two Dissociated Dislocations . . . . .	84
28	The Temperature Dependence of Shear Modulus . . . . .	92

LIST OF TABLES

<u>TABLE</u>		<u>Page</u>
1	Chemical Composition of Zircaloy . . . . .	2
2	Possible Thermally Activated Deformation Processes . . . . .	19
3	Hardening by Various Defects . . . . .	29
4	Possible Rate Controlling Mechanisms for hcp Metals . . . . .	33
5a	Deformation Behaviour of Zirconium . . . . .	34
5b	Deformation Behaviour of Zirconium-Oxygen Alloys . . . . .	35
6	Composition of Zircaloy-4 Sheet . . . . .	42
7	Annealing Treatment for Zr-4 and its Oxygen Alloys (0.12 - 1.00 Wt%O) . . . . .	44
8	Yield Strength Values for Zr-4 and its Oxygen Alloys (0.12 - 1.00 Wt%O) . . . . .	52
9a	$\tau^*$ Values Determined at the Plastic Strain of 1% for Zircaloy-4-Oxygen Alloys . . . . .	59
9b	$\tau^\mu$ Values Determined at the Plastic Strain of 1% for Zircaloy-4-Oxygen Alloys . . . . .	60
10	$V^*$ Values Determined by Strain Rate Change Tests for Zircaloy-4-Oxygen Alloys . . . . .	61
11	Values of $Q^*$ , $\alpha$ , $\Delta G^0$ and $\Delta G^\mu$ as a Function of Oxygen Content and Temperature . . . . .	64
12	$\Delta G^\mu$ Values for Zircaloy-4 and its Oxygen Alloys . . . . .	66
13a	$\Delta G^0$ Values Calculated on the Basis of Applied Stress $\tau$ . . . . .	75
13b	$\Delta G^\mu$ Values Calculated on the Basis of Applied Stress $\tau$ . . . . .	76

<u>TABLE</u>		<u>Page</u>
14	Comparison of the Theoretical Predictions from Specific Deformation Mechanisms with the Experimental Results . . . . .	82
15	The Comparison Between Observed and Calculated ' $\lambda$ ' Values at 600°C . . . . .	88

## 1. INTRODUCTION & OBJECTIVES

The first and foremost use of Zirconium, after its production started in 1948, has been in nuclear industry. In nuclear reactors (especially Light Water Reactors), Zirconium is used in the form of an alloy as a cladding tube material. The cladding tube in a reactor acts as a suitable container (1) for holding the atomic fuel and the highly radioactive fission products. It also isolates the fuel from its surroundings (e.g; coolant). The tube material must have adequate strength and ductility, good thermal conductivity, low neutron absorption cross-section and it should not react with the fuel and coolant. Zirconium is chosen as a tube material since it exhibits the above properties. Furthermore, the strength and corrosion behaviour of Zirconium are improved by the addition of tin and minor quantities of iron, nickel and chromium. This led to the development of Zr-2. The alloy Zr-2 was modified to Zr-4 by replacing nickel with an increased amount of iron. The (1) absence of nickel in Zr-4 reduces hydrogen pick-up and that reduces the hydride embrittlement of Zirconium. The nominal chemical composition of Zr-2 and Zr-4 are given in the following Table.

TABLE 1

Nominal Chemical Composition of  
Zircaloy (Wt%)

	<u>Sn</u>	<u>Fe</u>	<u>Cr</u>	<u>Ni</u>	<u>O</u>	<u>Zr</u>
Zr-2	1.5	0.12	0.10	0.05	0.1	bal
Zr-4	1.5	0.21	0.10	-	0.1	bal

Zirconium and its alloys have been studied in great detail for their mechanical properties, transformation characteristics and corrosion behaviour in the temperature range which includes both, below and above, the operating temperature for nuclear reactor (350°C - 450°C). However it is only recently, that embrittlement behaviour of cladding tube in case of loss-of-coolant accident (LOCA) has been under investigation and oxide embrittlement problem has been recognized as a serious problem similar to that of hydrogen embrittlement. Therefore any safety study on reactor should include the evaluation of deformation of fuel clad in the course of LOCA. This accident is caused by a rupture in the piping system of the primary coolant circuit and results in a rapid loss and pressure drop of the coolant followed by a rapid temperature rise of the fuel element sheath. This increase in temperature would enhance the oxidation rate of sheath and will also

cause oxygen content variation on the sheath depending upon the temperature. This warrants the study of the effects of oxygen on the high temperature mechanical properties of Zircaloy. At the same time it would be interesting to find out the role played by oxygen atoms in determining the deformation behaviour of Zircaloy. A temperature range of 600°C to 800°C was chosen for this study for the following reasons; (i) below 600°C, a considerable amount of information is available (2-15); and, (ii) at temperatures slightly above 800°C, Zirconium enters a two phase region, Figure 1 (16), and this could be studied only after a better understanding has been achieved for single phase material. Creep studies on this material in this temperature range have been reported by many authors (17 - 19), but the creep test data collected from such experiments suffer from a serious drawback as discussed by Lee and others (20). In creep tests, the data are obtained from separate tests and as such each point on a strain rate vs stress ( $\dot{\epsilon}$ - $\sigma$ ) curve represents a different strain history and a different structure. At the minimum creep rate the dislocation density ( $\rho$ ) has been shown to be proportional to applied stress ( $\sigma$ ) as  $\rho = A^n$  where A is constant and n varies with the temperature and material. The subgrain size developed at the end of primary creep is inversely proportional to stress. Therefore, the slope of the  $\sigma$ - $\dot{\epsilon}$  curve cannot be related to a specific metallurgical structure,

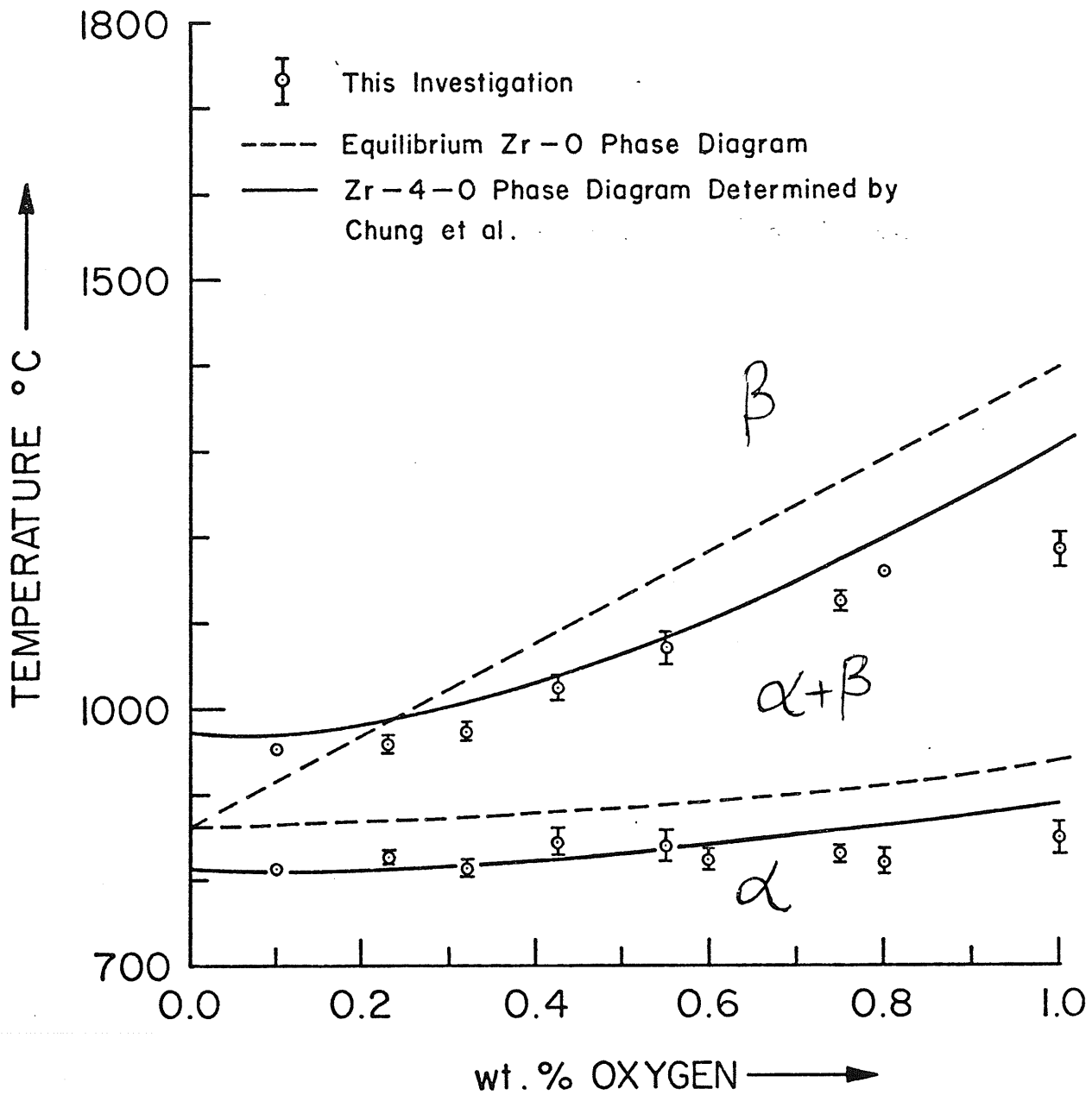


FIGURE 1. PSEUDOBINARY Zr-4-O PHASE DIAGRAM

in terms of, for example, dislocation density or substructure and has consequently no clear physical significance. On the other hand, the more suitable technique of stress and/or strain rate differential test could be employed to examine the stress dependence of strain rate for a given constant structure. The only precaution in the latter case should be that the accumulation of plastic strain is small or the test conditions are such that they produce negligible strain hardening. As such a great deal of tension (3,4) and compression (5) studies have been reported for polycrystalline Zirconium at elevated temperatures. However the effect of oxygen concentration on rate controlling dislocation mechanisms for Zirconium in this temperature range has been dealt by Mills and Craig (11) only. They employed the stress relaxation technique to calculate the activation volume and activation energy. The rate controlling mechanism in this temperature range for alloys was proposed to be the non-conservative motion of jogged screw dislocations (11). One of the characteristics of this mechanism is that the activation energy be equal to the self-diffusion energy of the material (Zirconium). However their results could be influenced by the recovery taking place during the stress relaxation tests. Furthermore, their activation energy values are in the range of 0.8 - 0.3 ev contrary to the self-diffusion energy value of 2.2 ev (21). Due to this discrepancy in energy values, Luton and Jonas have proposed



another mechanism for Zirconium (5) and Zirconium-tin alloys (22). According to them, the thermally activated event controlling the deformation is likely to be the break up of attractive junctions. Alloying of Zirconium causes the stability of attractive junctions probably due to the decrease in stacking fault energy (SFE) and thus requires a higher activation energy for break up of their junctions. However their results are based on the assumption of the yield stress as effective stress, which is not realistic. Thus a clear picture, in general about high temperature deformation behaviour of Zirconium is lacking.

The main aim of the project would thus be twofold; (i) Production of engineering data; e.g, yield strength and strain rate sensitivity for all alloys at all temperatures; (ii) The use of decremental unloading technique (first suggested by Gibbs [23]) to calculate the internal stress for all alloys. The thermal activation parameters (volume, energy) will then be calculated on the basis of effective stress (flow stress - internal stress) and these will be utilized to identify the dislocation mechanisms responsible for the deformation behaviour of these alloys.

## 2. LITERATURE SURVEY

### 2.1 Plastic Flow of Metals ( $0^{\circ}\text{K} - T_m^{\circ}\text{K}$ )

Plastic deformation is a consequence of the movement of dislocations through the crystal lattice under the action of an applied stress. The time dependent strain at constant temperature and constant stress, and the dependence of flow stress on the temperature and strain rate, confirm that the plastic flow is dynamic in nature (24). Becker recognized this dynamic nature of plastic deformation and proposed that thermal fluctuations assist the applied stress in overcoming obstacles for the flow of material. So the main task for a researcher lies in identifying the obstacles to the flow of material. These obstacles have a characteristic energy associated with them and their identification helps in determining the rate controlling dislocation mechanism or mechanisms. Figure 2 is a schematic diagram, showing the dependence of flow stress on temperature and strain rate for pure metals.

#### 2.1.1 Thermal and athermal obstacles

The obstacles to dislocation motion may be divided into two categories; short-range and long-range (25, 26).

- (a) In the case of short-range obstacles, the force required to overcome the barrier increases rapidly with the proximity of dislocation to the obstacle

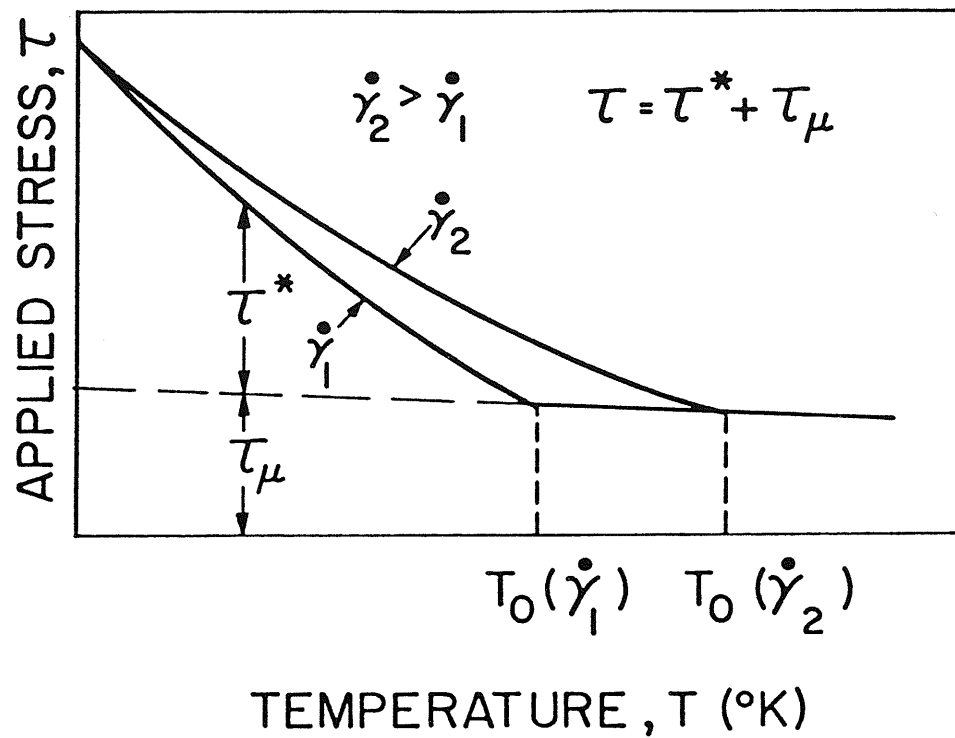


Fig. 2 . Schematic diagram showing the variation of the stress with temperature and strain rate and also the partition of thermal and athermal stress (27) .

and the stress field of such obstacles generally extends only over the order of several atomic distances. The interaction energy of these obstacles with dislocations is less than a few electron volts and hence these can be overcome with the aid of thermal fluctuations. So these are termed as thermal obstacles and the stress required to overcome these barriers is known as thermal or effective stress ( $\tau^*$ ). Generally, these obstacles in metals are due (26) to (i) P-N barrier; (ii) Forest dislocations; (iii) Motion of jogs in screw dislocation; (iv) cross-slip of screw dislocations; and, (v) climb of edge dislocations. The Peirel's-Nabarro stress, forest dislocations and jogs represent resistance to the motion of dislocations in the slip plane, while cross-slip and climb represent resistance to the motion of dislocations out of the slip plane.

- (b) In the case of long-range obstacles, the force required to overcome the barrier varies slowly with the dislocation position and the stress fields associated with these obstacles generally extend over a large distance within the crystal. Their interaction energy with the dislocation is so high that the thermal energy is insignificant as compared to that required by the dislocation to overcome them. These obstacles

are termed as athermal obstacles because of the weak dependence of their interaction energy on temperature and the stress required to overcome the barrier is known as athermal stress. Two common athermal obstacles are other dislocations on parallel slip planes and large precipitates or second phase particles. This stress is relatively temperature insensitive and depends on temperature only weakly through the temperature dependence of shear modulus. Figures 3(a) and 3(b) show both thermal and athermal stress fields (27) and their dependence on the spacing between dislocations and obstacles. In general, both types of obstacles are present in the lattice and the applied shear stress  $\tau$ , can be considered to consist of two components.

$$\tau = \tau_{\mu} + \tau^{*} \quad (1)$$

Where  $\tau_{\mu}$  is called the "athermal", "internal", "long-range" or "back" stress.  $\tau^{*}$  is the "thermal" or "effective" stress. This could be represented schematically in Figure 3(b) where at temperature 0°K, the total stress needed for plastic flow to occur would be  $\tau_0$ . However, the stress needed to initiate deformation would decrease with an increase in temperature. At any temperature, the stress would only be  $\tau$  because the rest of the resistance for dislocation motion is

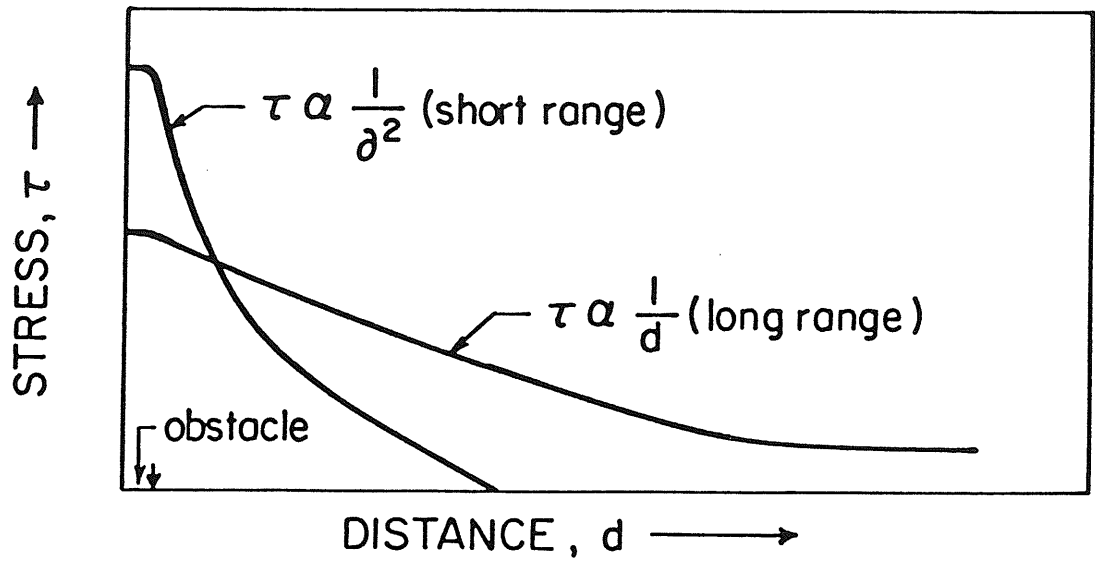


Fig 3(a) Stress - distance curves for typical long and short range interactions (27) .

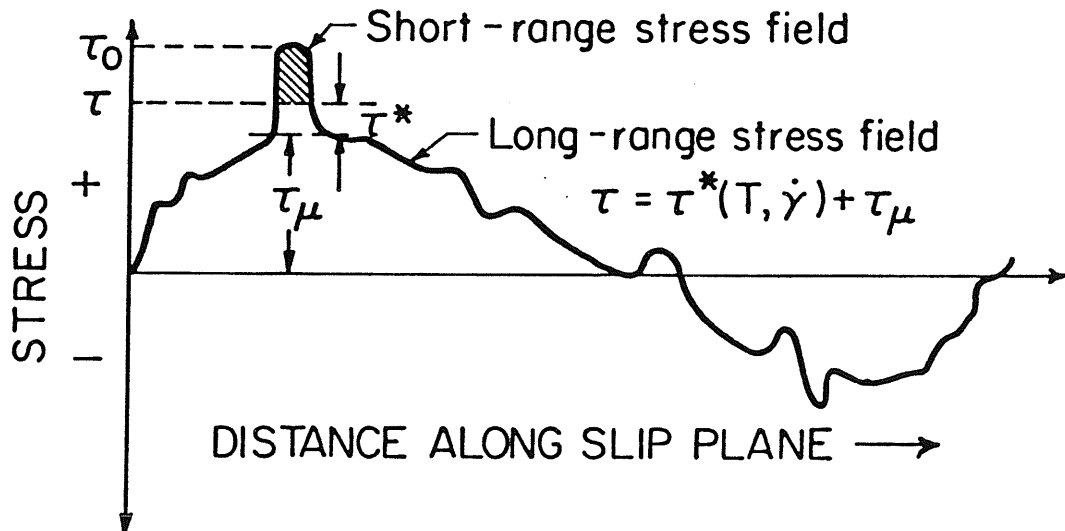


Fig 3(b) Schematic diagram illustrating long and short range stress fields encountered by a moving dislocation (27) .